

Elastic constants of incommensurate solid ^4He from diffusion Monte Carlo simulationsClaudio Cazorla,^{1,*} Yaroslav Lutsyshyn,² and Jordi Boronat³¹*Institut de Ciència de Materials de Barcelona (ICMAB-CSIC), 08193 Bellaterra, Spain*²*Institut für Physik, Universität Rostock, 18051 Rostock, Germany*³*Departament de Física i Enginyeria Nuclear, Universitat Politècnica de Catalunya, Campus Nord B4-B5, E-08034 Barcelona, Spain*

(Received 5 February 2013; revised manuscript received 7 May 2013; published 28 June 2013)

We study the elastic properties of incommensurate solid ^4He in the limit of zero temperature. Specifically, we calculate the pressure dependence of the five elastic constants (C_{11} , C_{12} , C_{13} , C_{33} , and C_{44}), longitudinal and transversal speeds of sound, and the $T = 0$ Debye temperature of incommensurate and commensurate hcp ^4He using the diffusion Monte Carlo method. Our results show that under compression, the commensurate crystal is globally stiffer than the incommensurate, however at pressures close to melting (i.e., $P \sim 25$ bar) some of the elastic constants accounting for strain deformations of the hcp basal plane (C_{12} and C_{13}) are slightly larger in the incommensurate solid. Also, we find that upon the introduction of tiny concentrations of point defects, the shear modulus of ^4He (C_{44}) undergoes a small reduction.

DOI: [10.1103/PhysRevB.87.214522](https://doi.org/10.1103/PhysRevB.87.214522)

PACS number(s): 67.80.—s, 02.70.Ss

I. INTRODUCTION

An intriguing resemblance between the dependence of the shear modulus (SM) and torsional oscillator (TO) frequency changes on the temperature, amplitude, and concentration of ^3He impurities has been experimentally observed in solid ^4He at low temperatures.¹ Crystal defects are clearly involved in both phenomena, however it remains a mystery how SM and TO fluctuations are exactly related. Day and Beamish identified the stiffening of solid helium with decreasing temperature, i.e., an increase of its shear modulus, with the pinning or unpinning of dislocations by isotopic impurities. Subsequent experiments have confirmed the interpretations of Day and Beamish,² although recent elasticity measurements on ultrapure single crystals seem to suggest that SM variations cannot be uniquely understood in terms of mobile dislocations.^{3,4}

Torsional oscillator anomalies were first interpreted as the mass decoupling of a certain supersolid fraction,^{5,6} a counterintuitive physical phenomenon that Andreev and Lifshitz already proposed in solid helium more than 40 years ago.⁷ Supporting this view is the fact that TO anomalies appear to occur only in bulk ^4He .⁸ Nevertheless, the supersolid interpretation of TO anomalies seems to leave open its connection to SM fluctuations, and diverse theoretical arguments and hypotheses have been put forward in an attempt to simultaneously rationalize the origins of both anomalies. Anderson, for example, proposes that supersolidity is an intrinsic property of bosonic crystals, which is only enhanced by disorder, and that the elastic anomaly is due to the generation of vortices at temperatures close to the supersolid transition.⁹ From a diametrically opposite standpoint, Reppy has argued that the TO behavior is caused by an increase of the ^4He shear modulus which mimics mass decoupling by stiffening the TO setup.¹⁰ Other scenarios somewhat more reconciling with the original TO and SM interpretations have also been proposed in which, for instance, mass superflow is assumed to occur in the core of dislocations only when these are static.^{4,11}

As can be appreciated, definitive conclusions on the roots of SM and TO anomalies remain contentious. In a recent paper, Chan *et al.*¹² have shown that for solid ^4He in vycor the nonclassical rotational inertia (NCRI) disappears if the TO setup is designed in such a way that it is completely free from any shear modulus stiffening effect. This result seems to show that NCRI can be totally attributed to elastic effects and not to the existence of a supersolid fraction.¹³ On the other hand, a recent experiment in which dc rotation was superposed to both TO and SM measures suggested that the cause of both anomalies below a critical temperature could have different microscopic origins.¹⁴ Also, the source of a small peak in the specific heat of ^4He (Ref. 15) at temperatures close to that at which TO and SM anomalies appear remains yet unexplained.

In this work, we study the change in the elastic constants of solid ^4He caused by the presence of small point defect concentrations, n_v , of 0.5–2.0%. As it has been shown, the presence of vacancies induces a finite superfluid fraction in the crystal (incommensurate crystal, IC)^{16,17} so that we can theoretically compare the elastic constants of a supersolid with those of the perfect crystal (commensurate crystal, C). In particular, we estimate the pressure dependence of the elastic constants C_{ij} 's (C_{11} , C_{12} , C_{13} , C_{33} , and C_{44} , where the last one is also known as the shear modulus) and derived quantities (the $T = 0$ Debye temperature and transverse or longitudinal speeds of sound) of bulk IC and C hcp ^4He . Our calculations show that (i) under moderate and large compressions, the C phase is globally stiffer than the IC solid, (ii) at pressures close to melting (i.e., $P \sim 25$ bar) some of the elastic constants accounting for specific strain deformations of the hcp basal plane (C_{12} and C_{13}) are slightly larger in the IC crystal, and (iii) the shear modulus difference between C and IC ^4He crystals is about 10 to 90 times smaller (in absolute value) than the experimentally observed C_{44} variation caused by the pinning or unpinning of dislocations.

The remainder of this article is organized as follows. In the next section, we briefly describe the computational methods employed and provide the details of our calculations. Next, we

present and discuss the results obtained, and we summarize the main conclusions in Sec. IV.

II. COMPUTATIONAL METHOD

In this study, we employ the diffusion Monte Carlo method (DMC), an accurate ground-state approach in which the Schrödinger equation of an N -particle interacting system is solved stochastically by simulating branching and diffusion processes in imaginary time.^{18,19} As is usual in DMC, we introduce a guiding wave function (GWF) for importance sampling that crucially reduces the variance of the statistical estimations. Our GWF model is symmetric under the exchange of atoms and correctly reproduces the experimental equation of state of solid ^4He and other quantum crystals.^{16,20,21} We note that DMC energies are virtually exact, i.e., they are only subjected to statistical bias, and ultimately they do not depend on the particular choice of the guiding wave function (as we have checked in the present study by conducting additional path-integral ground-state calculations in which a high-order short-time Green's function expansion has been used²²). The value of all technical parameters, i.e., the size of the simulation box, the population of walkers, and the length of the imaginary time step, have been set in order to ensure convergence of the total ground-state energy to less than 0.01 K/at (i.e., this is our typical statistical uncertainty). As in previous works, we modeled the ^4He - ^4He interactions with the Aziz II pairwise potential.²³ Further technical details of our elastic constant calculations can be found in Refs. 24 and 25.

It is important to stress that DMC C_{ij} estimations essentially rely on the computation of total energies (E) as a function of the strain (ϵ), in particular on the value of second derivatives

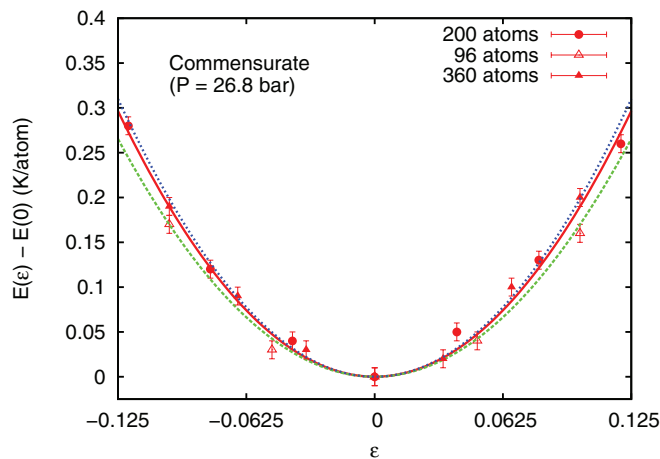


FIG. 1. (Color online) Effects of the size of the simulation box on the calculation of the second derivative of the total energy per atom, E , with respect to strain, ϵ (shear modulus case). The red solid, blue dotted, and green dashed lines correspond to parabolic fits performed on results obtained in 200-, 360-, and 96-atom simulation boxes, respectively. For comparison purposes, all the curves have been shifted to zero without any loss of generality (since we are mainly concerned with their curvature). 200- and 360-atoms parabolic fits are coincident within their statistical errors [i.e., $\partial^2 E / \partial^2 \epsilon = 19.0(5)$ and $19.8(5)$ K, respectively] in contrast to the 96-atom case [i.e., $17.0(5)$ K].

$\partial^2 E / \partial^2 \epsilon$,²⁴ and that numerical errors stemming from finite-size effects can already be made negligible in computationally affordable simulation boxes of $24.2 \text{ \AA} \times 24.2 \text{ \AA} \times 27.4 \text{ \AA}$ containing 200 atoms (see Fig. 1, where the results of a finite-size test performed in the commensurate phase are shown; analogous tests were carried out also in the incommensurate phase, and we arrived at the same conclusions).

Finally, the IC phase is built up by introducing small vacancy concentrations of 0.5–2.0% in the crystal. Although it is well known that the presence of point defects in solid ^4He is energetically penalized,^{26,27} this route allows for simulation of supersolids under tight and controllable conditions.^{25,28–31} On the technical side, superfluid fractions, ρ_s / ρ , were obtained from the diffusion of the center of mass of crystals computed at very long imaginary times.^{21,32} Small variations in our ρ_s / ρ results would essentially not alter the conclusions that we present next.

III. RESULTS AND DISCUSSION

In Fig. 2, we show the shear modulus of C and IC (with $\rho_s / \rho = 2\%$) hcp ^4He expressed as a function of pressure. We find that in both states, C_{44} behaves linearly with pressure over the entire range of densities considered, i.e., $0.028 \leq \rho \leq 0.033 \text{ \AA}^{-3}$. As one may also see, the shear modulus of the C crystal is larger than that of the IC solid, and the value of the $\Delta C_{44} \equiv C_{44}^C - C_{44}^{\text{IC}}$ difference increases under compression. It must be noted that the numerical uncertainty in our C_{44} calculations is 5 bar, thus the predicted ΔC_{44} values are rigorously different from zero at pressures above 50 bar (see Fig. 4).

In principle, one may expect that in addition to pressure, ΔC_{44} variations are also dependent on the imposed fraction of mass superflow, or conversely, the concentration of point defects. However, as we show in Fig. 3, such a dependence turns out to be rather weak. For instance, in the $0 \leq \rho_s / \rho \leq 3\%$ interval, C_{44} decreases in less than 5% of its ground-state value, and even when an excessive

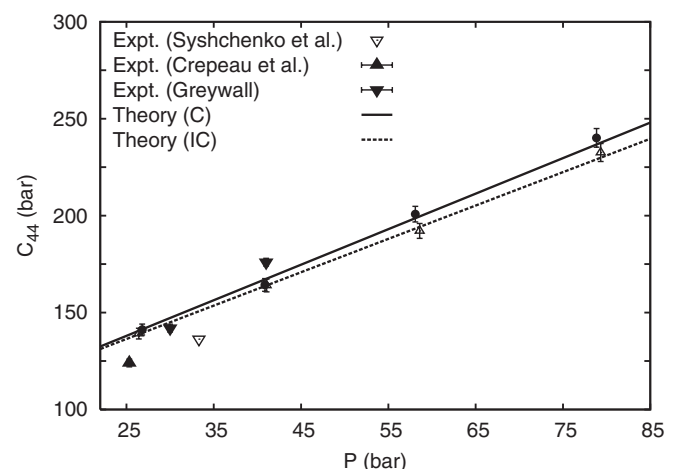


FIG. 2. Shear modulus results obtained for C and IC hcp ^4He expressed as a function of pressure. Experimental data from Refs. 36, 38, and 39 are shown for comparison. Solid lines represent linear fits to DMC results (see text).

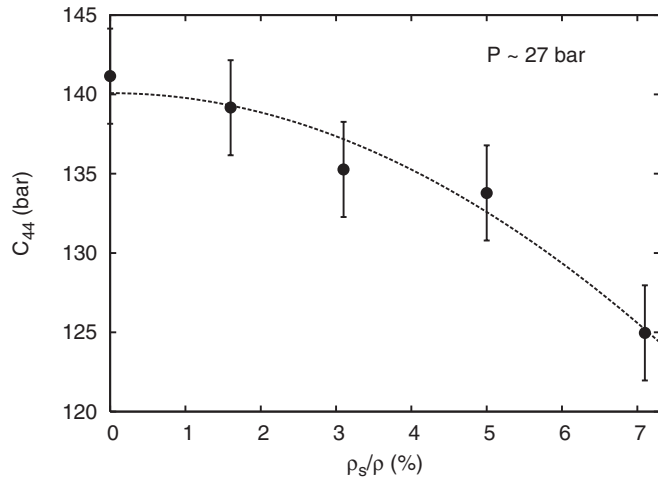


FIG. 3. The shear modulus of IC solid hcp ^4He expressed as a function of the superfluid fraction at pressures close to melting. The dashed line is a guide to the eyes.

ρ_s/ρ value of 7% is constrained the accompanying variation of shear modulus is of just $\sim -11\%$. Concerning possible temperature effects, it is well known that the contribution of phonon excitations to the thermal energy of solids reduces the speeds of sound by an amount that is proportional to T^4 , thus implying a $\propto T^8$ dependence in the elastic constants.³³ Our zero-temperature conclusions on ΔC_{44} , therefore, can be fairly generalized to the regime of ultralow temperatures (that is, few mK). In fact, the ground-state results reported in this study are in very good agreement with those obtained by Ardila *et al.* for hcp ^4He at $T = 1$ K using the path-integral Monte Carlo method,³⁴ and by

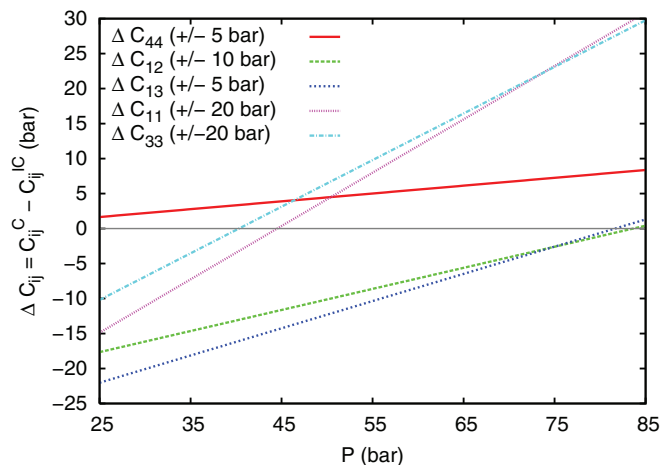


FIG. 4. (Color online) Elastic constant differences between C and IC crystals ($\rho_s/\rho = 2\%$) of hcp ^4He expressed as a function of pressure. The size of the error bars is indicated within the parentheses. Positive ΔC_{ij} values indicate softening of the corresponding elastic constant in a hypothetical vacancy-induced normal-to-supersolid phase transition.

Pessoa *et al.* at zero temperature using the variational Monte Carlo approach.³⁵

It must be stressed that our C_{44} results are obtained for pure ^4He single crystals, i.e., zero concentration of ^3He atoms and free-of-dislocations, hence direct comparisons to Day and Beamish^{1,2,36} data obtained in polycrystals turn out to be very complicated. In light of our results, however, one may notice that experimentally observed shear modulus variations caused by the pinning or unpinning of dislocations are of opposite sign and about one order of magnitude larger (10–20% in polycrystals and ~ 50 –90% in monocrystals³⁷) than fluctuations reported here for hypothetical superfluid mass flows of $\sim 1\%$ (see Fig. 3). Consequently, we may conclude that if a vacancy-induced normal-to-supersolid phase transition occurred in solid helium, then dislocation-mediated mechanical contributions to C_{44} would totally overwhelm those stemming from mass superflow. Interestingly, Rojas *et al.* have recently reported an anomalous softening of high-quality ultrapure monocrystals in the temperature region wherein supersolidity could occur.⁴

We have also determined the $\Delta C_{ij}(P)\{ij = 11, 12, 13, 33\}$ deviations describing the response of C and IC hcp crystals to strain basal plane deformations.²⁴ First, we note that all these components also present a linear dependence on pressure (see Fig. 4, where numerical uncertainties are indicated within parentheses). Second, ΔC_{ij} slopes are all positive, thus implying that beyond a certain critical pressure, C hcp ^4He is plainly stiffer than the IC crystal. According to our calculations, this critical pressure is above 85 bar. Interestingly, C_{12} and C_{13} are largest, by a small amount, in the IC solid at pressures below 50 and 70 bar, respectively. This outcome shows that in a hypothetical low-pressure normal-to-supersolid phase transition, the final supersolid could behave more rigidly than the initial normal state under certain strain deformations. Nevertheless, we find that the C_{66} coefficient, which is defined as $\frac{1}{2}(C_{11} - C_{12})$ and can be directly measured in acoustic experiments, is always smaller in the IC state. This behavior is analogous to the tendency found for the shear modulus, although C_{66} variations are in general larger (e.g., at $P = 25$ bar, $\Delta C_{66} \approx \Delta C_{44}$, whereas at $P = 85$ bar, $\Delta C_{66} \approx 2\Delta C_{44}$).

Finally, Fig. 5 shows the calculated longitudinal and transversal speeds of sound (v_L and v_T) of C and IC hcp ^4He under pressure.²⁴ As one can observe, v_L velocities along the hcp c axis and basal plane are slightly larger in the IC crystal within approximately the same pressure range in which ΔC_{12} and ΔC_{13} deviations are found to be negative. Nevertheless, speeds of sound deviations near melting turn out to be so small that in practice these could probably not be detected with standard means. The same can be concluded about the $T = 0$ Debye temperature for which, as we show in Fig. 5, the corresponding C-to-IC variation is smaller than the typical experimental precision. In view of these technical limitations, it would be very interesting to perform new C_{ij} and $v_{L,T}$ measurements on ^4He at large pressures (i.e., $P \geq 60$ bar) where larger C-to-IC differences develop. In this regard, spectroscopic measurements of the E_{2g} phonon mode (i.e., the shear mode corresponding to the beating of the two hcp sublattices against each other in the two orthogonal directions

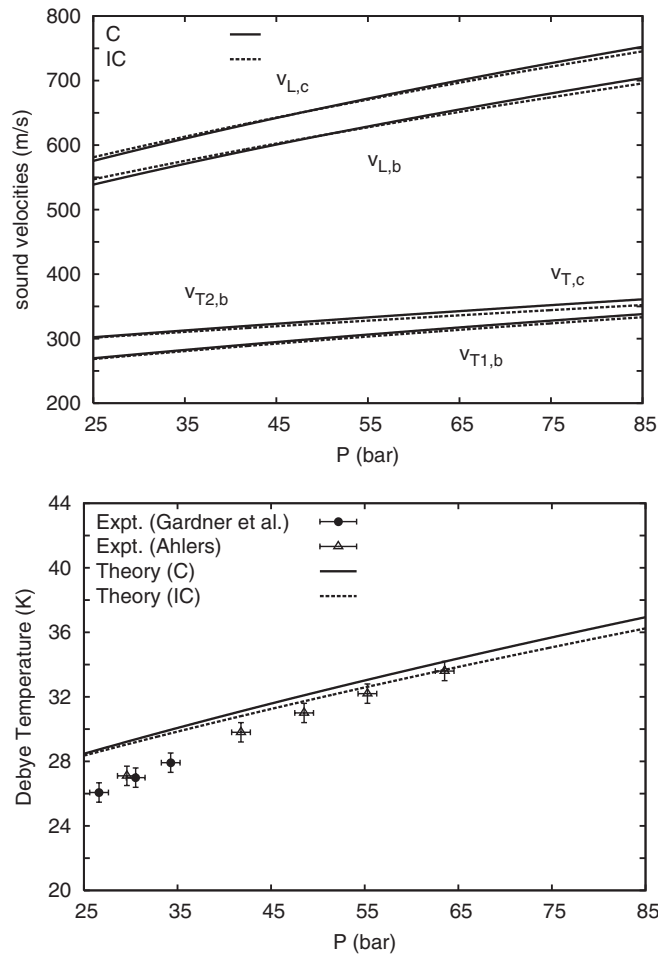


FIG. 5. Top: Calculated longitudinal (L) and transverse (T) speeds of sound along the basal plane (b) and c axis (c) of C and IC ($\rho_s/\rho = 2\%$) hcp ^4He as a function of pressure. Bottom: Estimated $T = 0$ Debye temperature of C and IC hcp ^4He as a function of pressure. Experimental data from Refs. 40 and 41 are shown for comparison.

of the basal plane) would be particularly helpful since in this type of experiment, (i) C_{ij} values can be determined with a very small imprecision of less than the 2%, (ii) tiny solid samples are needed (i.e., of μm size), thus likely crystal quality issues present in SM and TO experiments could be somehow alleviated, and (iii) pressure conditions can be efficiently tuned.⁴²

IV. CONCLUSIONS

To summarize, we have studied the elastic properties of hcp solid ^4He in a metastable IC state and compared them to those obtained for its C ground state. Our calculations show that near melting elastic constants C_{11} and C_{12} accounting for specific strain deformations of the hcp basal plane are slightly larger in the IC crystal. At moderate and high pressures, however, the C phase is always stiffer than the IC. Also, we find that the appearance of a finite superfluid fraction (e.g., $\rho_s/\rho \sim 1\%$) caused by the introduction of vacancies unequivocally provokes a small decrease of the ^4He shear modulus (i.e., $\Delta C_{44} \sim 1\%$). We argue then that if a vacancy-induced normal-to-supersolid phase transition occurred in helium crystals containing isotopic impurities and line defects, dislocation-mediated contributions to C_{44} would totally overwhelm those stemming from mass superflow. As an alternative to usual dynamic experiments focused on the search of hypothetical supersolid manifestations, we suggest to perform spectroscopic measurements of the E_{2g} mode of ^4He at moderate and high pressures.

ACKNOWLEDGMENT

This work was supported by MICINN-Spain Grants No. MAT2010-18113, CSD2007-00041, and FIS2011-25275, and Generalitat de Catalunya Grant No. 2009SGR-1003.

*ccazorla@icmab.es

¹J. Day and J. Beamish, *Nature (London)* **450**, 853 (2007).

²J. Day, O. Syshchenko, and J. Beamish, *Phys. Rev. B* **79**, 214524 (2009).

³X. Rojas, C. Pantalei, H. J. Maris, and S. Balibar, *J. Low Temp.* **158**, 478 (2009).

⁴X. Rojas, A. Haziot, V. Bapst, S. Balibar, and H. J. Maris, *Phys. Rev. Lett.* **105**, 145302 (2010).

⁵E. Kim and M. H. W. Chan, *Nature (London)* **427**, 225 (2004).

⁶E. Kim and M. H. W. Chan, *Science* **305**, 1941 (2004).

⁷A. F. Andreev and I. M. Lifshitz, *Sov. Phys. -JETP* **29**, 1107 (1969).

⁸E. Kim, J. S. Xia, J. T. West, X. Lin, A. C. Clark, and M. H. W. Chan, *Phys. Rev. Lett.* **100**, 065301 (2008).

⁹P. W. Anderson, *Nat. Phys.* **3**, 160 (2007); *Phys. Rev. Lett.* **100**, 215301 (2008); *Science* **324**, 631 (2009).

¹⁰J. D. Reppy, *Phys. Rev. Lett.* **104**, 255301 (2010).

¹¹S. Balibar, *Nature (London)* **464**, 176 (2010).

¹²D. Y. Kim and M. H. W. Chan, *Phys. Rev. Lett.* **109**, 155301 (2012).

¹³J. R. Beamish, A. D. Fefferman, A. Haziot, X. Rojas, and S. Balibar, *Phys. Rev. B* **85**, 180501(R) (2012).

¹⁴H. Choi, D. Takahashi, K. Kono, and E. Kim, *Science* **330**, 1512 (2010).

¹⁵X. Lin, A. Clark, and M. Chan, *Nature (London)* **449**, 1025 (2007).

¹⁶C. Cazorla, G. E. Astrakharchick, J. Casulleras, and J. Boronat, *New J. Phys.* **11**, 013047 (2009).

¹⁷D. E. Galli and L. Reatto, *Phys. Rev. Lett.* **96**, 165301 (2006).

¹⁸J. Boronat and J. Casulleras, *Phys. Rev. B* **49**, 8920 (1994).

¹⁹C. Cazorla and J. Boronat, *J. Phys.: Condens. Matter* **20**, 015223 (2008).

²⁰C. Cazorla and J. Boronat, *Phys. Rev. B* **78**, 134509 (2008).

²¹C. Cazorla, G. E. Astrakharchick, J. Casulleras, and J. Boronat, *J. Phys.: Condens. Matter* **22**, 165402 (2010).

²²R. Rota, J. Casulleras, F. Mazzanti, and J. Boronat, *Phys. Rev. E* **81**, 016707 (2010).

- ²³R. A. Aziz, F. R. W. McCourt, and C. C. K. Wong, *Mol. Phys.* **61**, 1487 (1987).
- ²⁴C. Cazorla, Y. Lutsyshyn, and J. Boronat, *Phys. Rev. B* **85**, 024101 (2012).
- ²⁵R. Rota, Y. Lutsyshyn, C. Cazorla, and J. Boronat, *J. Low Temp. Phys.* **168**, 150 (2012).
- ²⁶D. M. Ceperley and B. Bernu, *Phys. Rev. Lett.* **93**, 155303 (2004).
- ²⁷M. Boninsegni, A. B. Kuklov, L. Pollet, N. V. Prokof'ev, B. V. Svistunov, and M. Troyer, *Phys. Rev. Lett.* **97**, 080401 (2006).
- ²⁸R. Rota and J. Boronat, *Phys. Rev. Lett.* **108**, 045308 (2012).
- ²⁹Y. Lutsyshyn, C. Cazorla, G. E. Astrakharchik, and J. Boronat, *Phys. Rev. B* **82**, 180506(R) (2010).
- ³⁰Y. Lutsyshyn, C. Cazorla, and J. Boronat, *J. Low Temp. Phys.* **158**, 608 (2010).
- ³¹Y. Lutsyshyn, R. Rota, and J. Boronat, *J. Low Temp. Phys.* **162**, 455 (2011).
- ³²S. Zhang, N. Kawashima, J. Carlson, and J. E. Gubernatis, *Phys. Rev. Lett.* **74**, 1500 (1995).
- ³³J. Beamish, *J. Low Temp. Phys.* **168**, 194 (2012).
- ³⁴L. A. P. Ardila, S. A. Vitiello, and M. de Koning, *Phys. Rev. B* **84**, 094119 (2011).
- ³⁵R. Pessoa, S. A. Vitiello, and M. de Koning, *Phys. Rev. Lett.* **104**, 085301 (2010).
- ³⁶O. Syshchenko, J. Day, and J. Beamish, *J. Phys.: Condens. Matter* **21**, 164204 (2009).
- ³⁷A. D. Fefferman, X. Rojas, A. Haziot, S. Balibar, J. T. West, and M. H. W. Chan, *Phys. Rev. B* **85**, 094103 (2012).
- ³⁸R. H. Crepeau, O. Heybey, D. M. Lee, and S. A. Strauss, *Phys. Rev. A* **3**, 1162 (1971).
- ³⁹D. S. Greywall, *Phys. Rev. A* **3**, 2106 (1971); *Phys. Rev. B* **16**, 5127 (1977).
- ⁴⁰W. R. Gardner, J. K. Hoffer, and N. E. Phillips, *Phys. Rev. A* **7**, 1029 (1973).
- ⁴¹G. Ahlers, *Phys. Rev. A* **2**, 1505 (1970).
- ⁴²J. Eckert, W. Thomlinson, and G. Shirane, *Phys. Rev. B* **18**, 3074 (1978).